Integration of waveguide type wavelength demultiplexing photodetectors by selective intermixing of InGaAs/InGaAsP quantum well structure

Deok Ho Yeo*, Kyung Hun Yoon, Hang Ro Kim, Sung June Kim

School of electrical engineering, Seoul national university, Seoul, Korea,

ABSTRACT

Wavelength demultiplexing photodetectors was fabricated using selective intermixing of InGaAs/InGaAsP multi-quantum well (MQW) structure. An InGaAs/InGaAsP MQW with u-InP cladding layer and u-InGaAs cap layer grown by metal organic chemical vapor deposition (MOCVD) was used for this experiment. Intermixing of InGaAs/InGaAsP MQW structure was done by a rapid thermal annealing after depositing SiO_2 dielectric layer on the InGaAs cap layer by plasma-enhanced chemical vapor deposition (PECVD). Three sections of shorter-wavelength PD, absorber region and longer-wavelength PD lined up linearly and the front two regions were intermixed. Output current ratios of fabricated photodetectors at wavelengths of 1550 and 1480 nm were about 20 dB and thus the photodetectors were proven to demultiplex both wavelengths.

Keywords: Quantum well intermixing, InGaAs/InGaAsP multi-quantum wells, dielectric cap annealing, dual wavelength photodetector, wavelength demultiplexing, waveguide type photodetector, integrated optics

1. INTRODUCTION

Photodetectors with a wavelength demultiplexing function is predicted to play an important role in future fiber optic communication system utilizing wavelength division multiplexing (WDM). To have such operation, hybrid integration of devices on planar lightwave circuit (PLC) technique[1] or monolithic integration of devices is possible[2-5]. PLC can utilize well made devices and can have good quality, but the system becomes bulky as compared to monolithic integration. Monolithic integration of devices is expected to bring about cost reduction and packaging robustness associated with replacing individual alignment, single-mode optical connections between discrete optoelectronic devices with lithographically produced integrated waveguides. There have been several reports on integration of wavelength demultiplexing detectors. A demultiplexing photodetector fabricated using Ar laser-assisted metal organic molecular beam epitaxy (MOMBE) has been reported[3]. In the Ar laser-assisted MOMBE growth, there are changes in growth rate and composition in laser focused area thus it has different bandgap energies. Tunable superlattice pin photodetector using the quantum confined Stark effect (QCSE) has been reported[4]. By varying applied voltages to the photodetector that has quantum well structure inside, changes in band-to-band transition energy can be obtained. Selective intermixing of quantum well structure can also be applied to demultiplexing photodetectors. Waveguide type InGaAs/GaAs metal-semiconductor-metal (MSM) demultiplexing photodetector using selective bandgap tuning has been reported[5].

Among the above techniques, quantum well intermixing can change confined bandgap energy of the quantum well easily and can produce large bandgap shift. This technique can be applied to fabrication of optical waveguides, wavelength shifted laser diode, and monolithic optoelectronic ICs. The intermixing technique renders the fabrication process easier than the epitaxial regrowth technique when different bandgap material is needed on the wafer. Various techniques such as ion implantation, Zn diffusion, pulsed laser irradiation, and impurity free vacancy diffusion using dielectric cap annealing have been developed for GaAs- or InP-based MQW structures. Intermixing of InP-based MQWs is particularly important because of their potential application at high capacity, and in long haul fiber optic communication systems. We have, recently, used a SiO_2 dielectric film on an InGaAs cap layer to promote the intermixing of an InGaAs/InP MQW system. MQWs annealed with a SiO_2 dielectric film on an InGaAs cap layer showed large blue shifts in photoluminescence spectrum and compositional mixing at the MQW region[6-7]. Applying this methods to an InGaAsP/InP MQW system, the spatial resolution of the IFVD process was found to be less than 3 μm. In our previous study, group III and V elements of MQW interdiffused at a similar rate after quantum well intermixing and this can reduce the separation between electron-heavy hole and electron-light hole transition energy in the MQW. Ridge-type waveguides were fabricated and showed large propagation loss reduction at the original bandgap after quantum well intermixing. In accordance with our previous results, we report, in

* E-mail: ydh@helios.snu.ac.kr; WWW:http://helios.snu.ac.kr; Telephone: 82-2-880-5451(ext.236); Fax: 82-2-887-6575

In *Optoelectronic Materials and Devices II*, Yan-Kuin Su, Pallab Bhattacharya, Editors,
Proceedings of SPIE Vol. 4078 (2000) • 0277-786X/00/$15.00

this paper, the integration of wavelength demultiplexing photodetectors using selective intermixng of InGaAs/InGaAsP MQW structure.

2.EXPERIMENTAL METHODS AND DEVICE FABRICATION

An InGaAs/InGaAsP MQW grown by metal organic chemical vapor deposition (MOCVD) was used for this experiment. The epitaxial layer structure was grown on an n-InP (Sn-doped; $1\times10^{18}cm^{-3}$) substrate and had included a 1㎛ S-doped n-InP buffer, a 0.15㎛ u-$In_{0.85}Ga_{0.15}As_{0.3}P_{0.7}$, a 0.05㎛ u-$In_{0.81}Ga_{0.19}As_{0.43}P_{0.57}$ confinement layer on both sides of the MQW, a 0.5㎛ u-InP cladding layer and a 0.1㎛ u-$In_{0.53}Ga_{0.47}As$ cap layer. The MQW structure consists of five layers of 84 Å $In_{0.53}Ga_{0.47}As$ and four layers of 100 Å $In_{0.77}Ga_{0.23}As_{0.47}P_{0.53}$. The epitaxial layers were intentionally undoped to avoid impurity induced disordering by Zn diffusion during the intermixing process and electrical isolation between devices. For the as-grown epitaxial layer, the PL peak wavelength of the MQW was found to be 1480 nm at 10 K and 1588 nm at room temperature. A 1700 Å SiO_2 dielectric layer was deposited on the InGaAs cap layer by plasma-enhanced chemical vapor deposition (PECVD) to enhance the intermixing of the MQW. To observe SiO_2 dielectric layer on InGaAs cap layer and annealing effect, bandgap energy shifts as a function of annealing time at a temperature of 750℃ was measured as shown in Fig. 1. Samples with and without SiO_2 dielectric layer on InGaAs cap layer were mounted on a rapid thermal annealer (RTA) and heated in N_2 environment. Bandgap shifts as large as 82 meV can be found upon annealing for 60 sec with SiO_2 dielectric layer. However, small shifts due to self-diffusion of MQW at high temperature were found for the samples without SiO_2 dielectric layer. Thus using the deposition and patterning of SiO_2 dielectric layer on InGaAs cap layer, different bandgap energies on one chip can be made.

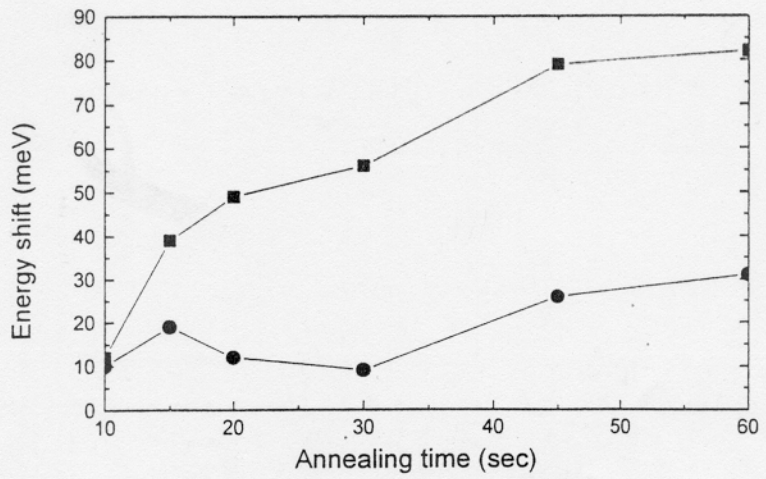

Fig. 1. Bandgap energy shifts of a MQW structure as a function of annealing time at a temperature of 750℃. Squares and circles denote bandgap energy shifts with and without SiO_2 dielectric layer on InGaAs cap layer, respectively.

From the above bandgap shift data, annealing at 750℃ for 45 s was adopted for the device fabrication because of the relatively large bandgap difference for the samples with and without SiO_2 dielectric on InGaAs cap layer. SiO_2 dielectric layer was selectively patterned using photolithography and wet chemical etch and the sample was mounted carefully on a rapid thermal annealer (RTA) and heated for 45 s in N_2 environment at 750℃. Figure 2 shows normalized

photoluminescence (PL) spectrums at 10 K for the MQWs, as-grown and annealed with and without SiO_2 dielectric layer. The full-width at half maximum (FWHM) of the PL spectrum remains nearly constant for the intermixed MQW demonstrating that the quality of the epitaxial layer was not significantly degraded after the intermixing process. MQW annealed without SiO_2 dielectric layer show a slight increase in bandgap in comparison with that annealed without SiO_2 dielectric layer. This is due to self-diffusion of well and barrier materials at high annealing temperature. Regions with and without SiO_2 dielectric layer had bandgap shifts of 26 and 79 meV and the bandgap difference between the two regions was 53 meV.

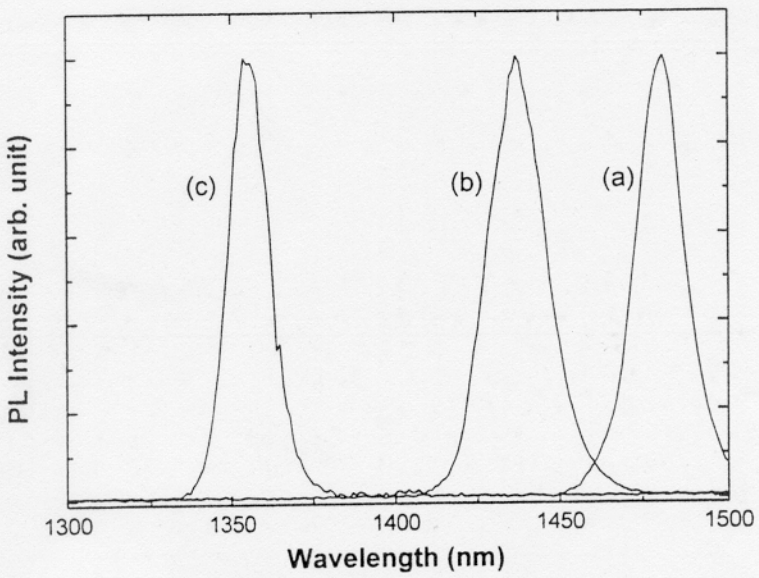

Fig. 2. Normalized PL spectrum of (a) as-grown , (b) annealed without SiO_2 and (c) with SiO_2 dielectric on InGaAs cap layer.

Figure 3 shows the device structure used in this work. Regions for shorter wavelength detection, dummy waveguide and longer wavelength are linearly lined up and coupled light propagates each region through 20 μmwide rib waveguide. The width of waveguide is 20 μm and the length of each detector is 250 μm. 1700 Å SiO_2 dielectric layer was deposited on the wafer by PECVD and patterned using photolithography and wet chemical etch. Regions for shorter wavelength detection and waveguide are annealed with SiO_2 dielectric layer and that for longer wavelength was annealed without it. After annealing, SiO_2 dielectric layer was removed by wet chemical etching. InGaAs cap layer between two detectors was wet chemically removed to reduce propagation loss. P-ohmic layer was formed at the contact region by Zn_3P_2 evaporation and annealing so that two photodetectors can be isolated electrically. Rib waveguide was formed by wet etch and SiO_2 dielectric layer was deposited by PECVD for the passivation layer. Au/AuZn/Cr/Au and AuGe/Ni/Au multi-level systems were used for P- and N-type contact metal.

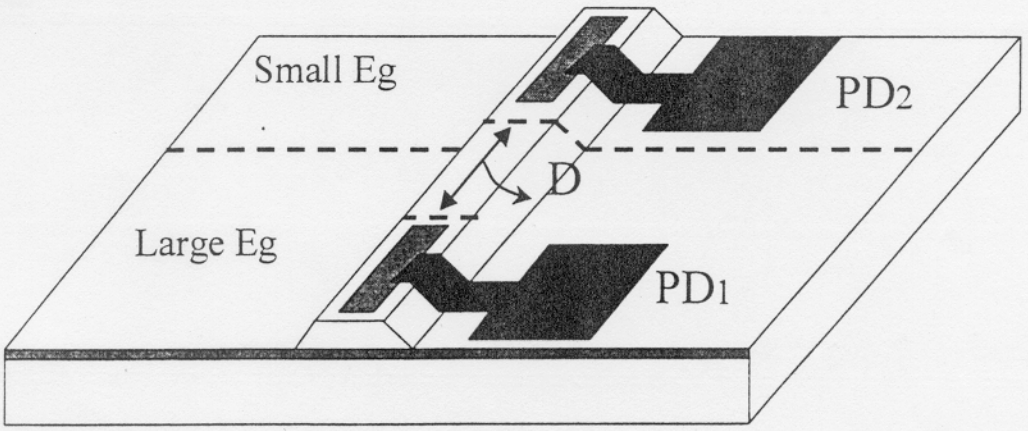

Fig. 3. Schematic diagram of integrated waveguide type photodetectors. Large bandgap area was annealed with SiO_2 dielectric layer on InGaAs cap layer.

3. MEASUREMENTS OF SPECTRAL RESPONSE

The detector response was characterized using tunable laser. We used two tunable lasers to obtain wide spectral range and as a result we could have wavelength range from 1480 to 1625 nm. Light was end-fiber coupled into the photodetector and the input polarization was set to TE or TM mode by polarization controller and the detector was zero biased. Figure 4 shows measured photocurrent spectrum of each detector for the polarization of TE/TM mode, respectively. Photocurrent was slightly reduced near 1480 nm due to instability of tunable laser light source. Photocurrent spectrum of PD_1 with larger bandgap energy shows blue shift with respect to that of PD_2 with smaller bandgap energy as is expected from PL measurements. For the photocurrent of TE mode, weak exciton peaks related to electron-heavy hole transition is seen at 1560 and 1490 nm for PD_1 and PD_2 respectively. Exciton peaks related to electron-light hole can not be seen because calculated transition occurs at a shorter wavelength than 1480 nm.

For a multi-segment waveguide photodetector, the photocurrent generated in segment i of length Li can be expressed as[8]

$$Ii = (\frac{e\lambda}{hc}) P_0 \gamma (1-R) \eta \frac{\Gamma \alpha_i^{int}(\lambda)}{\alpha_i(\lambda)} e^{-\sum_{k=1}^{i-1} \alpha_k(\lambda) L_k} (1 - e^{-\alpha_i(\lambda) L_i}) \qquad (1)$$

where $e\lambda/hc$ is the conversion factor from optical power to photocurrent, P_0 is the input optical, γ is the coupling efficiency, R is the reflectance at the waveguide facet, η is the internal quantum efficiency, Γ is the optical confinement factor of the active layer, $\alpha_i^{int}(\lambda)$ is the interband absorption coefficient in the segment i, and $\alpha_i(\lambda)=\Gamma\alpha_i^{int}(\lambda)+\alpha_0$ is the total attenuation coefficient in the segment $_i$, where α_0 is the scattering loss coefficient of the waveguide. For the waveguide photodetector, α_0 is a negligible effect. From eq. 1, light coupled to PD1 propagates through waveguide and its intensity decreases due to absorption and propagation loss in the MQW. Non-absorbed light from PD_1 and absorber region propagates to PD_2.

Figures 5 and 6 shows normalized photocurrent spectrum of integrated wavelength demultiplexing photodetectors for the TE and TM mode, respectively. Generated photocurrent spectrum of PD_1 will be same as figure 4 but that of PD_2 will be deformed. As can be seen in eq. 1, the amount of photons that reaches PD_2 region will be reduced as that absorbed and scattered in previous region. So the photocurrent of PD_2 at short wavelength decreases and that of long wavelength is unchanged. Photocurrent of PD_1 reduced to almost zero wavelength over 1570 nm and peak of photocurrent in spectral response of PD_2 is near 1570 nm.

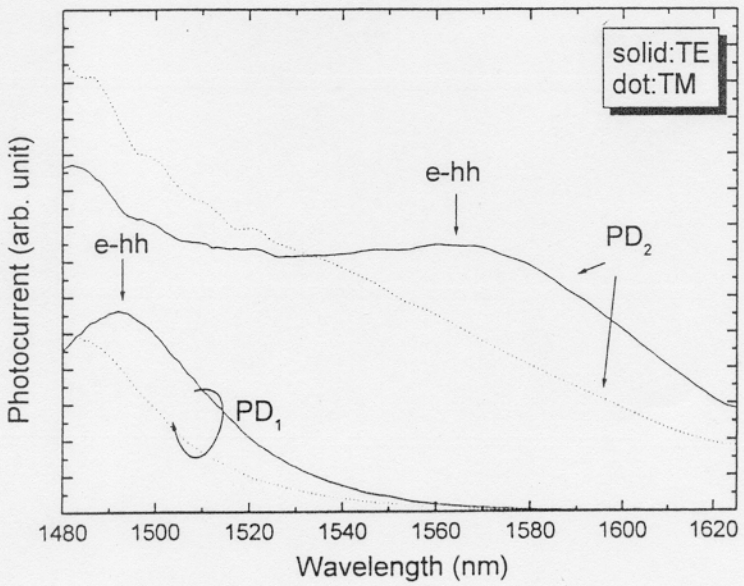

Fig. 4. Photocurrent spectra of fabricated photodetectors. Solid and dot line shows photocurrent spectrum for TE and TM mode, respectively.

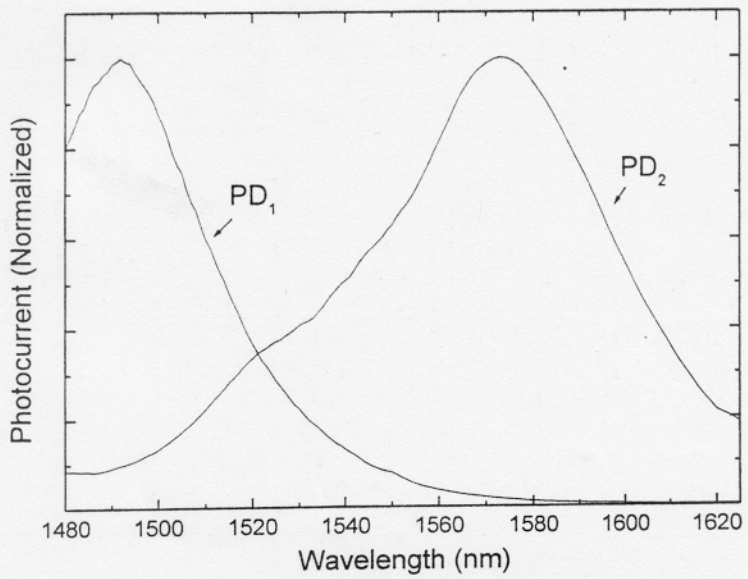

Fig. 5. Photocurrent spectra of integrated waveguide photodetectors for TE mode.

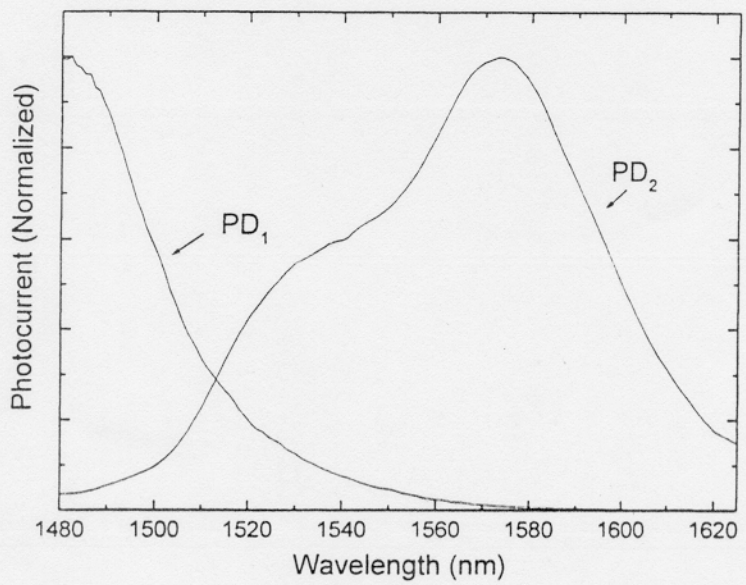

Fig. 6. Photocurrent spectra of integrated waveguide photodetectors for TM mode.

The crosstalk for the TE and TM mode light at short wavelength is due to incomplete absorption at PD_1. This results also from the scattered and unguided light that can reach PD_2 and generate photocurrent. For 100 μm dummy waveguide, photocurrent ratio of PD_1 and PD_2 was 4 to 1 at a wavelength of 1480 nm. Increasing the spacing between two photodetectors will reduce this crosstalk. Figure 7 shows the photocurrent ratio at 1477 nm changes as a function of the spacing between photodetectors. Light from DFB laser diode was coupled to the wavelength demultiplexing photodetectors and the light is attenuated at the waveguide. As can be expected from eq. 1, the photocurrent of the PD2 will be decreased exponentially and the ratio of PD1 to PD2. Solid line in the Fig. 7 Shows fitted line as an exponent function. For the waveguide 900 μm long, the ratio was about 200. The photocurrent ratio at 1550 nm was about 200 (~23 dB) irrespective of waveguide length. This is because light at this wavelength has small propagation loss through waveguide and a small fraction of the light was absorbed at PD_1. Thus it can be said that the fabricated device can demultiplex both 1480 and 1550 nm wavelength.

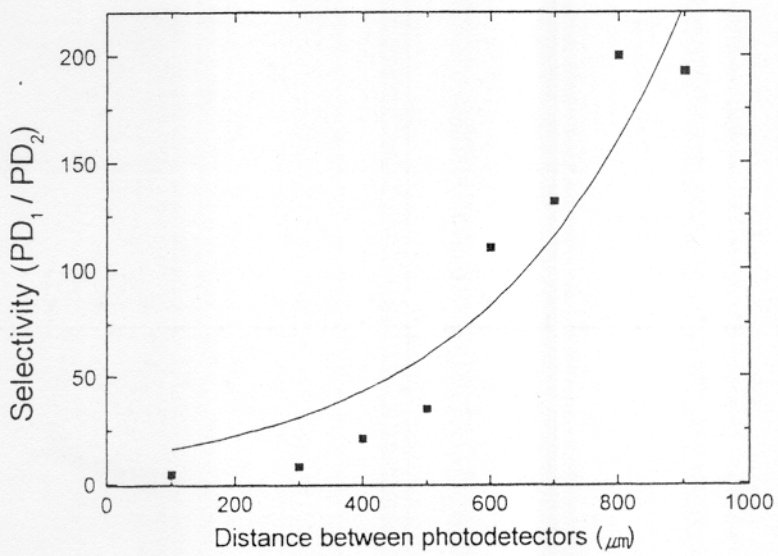

Fig. 7. Current ratio of PD_1 and PD_2 when the wavelength of coupled light was 1477 nm. Solid line shows exponential fitting curve.

4.CONCLUSION

A simple and effective fabrication method for producing two wavelengths demultiplexing p-i-n waveguide type photodetector was demonstrated. Selective area intermixing of InGaAs/InGaAsP MQW structure by SiO_2 dielectric cap annealing was used in the fabrication process. Large bandgap difference was seen in the wafer with and without by SiO_2 dielectric cap annealing. Spectral response of integrated photodetectors was measured for the wavelength range of 1480 to 1625 nm. Photodetectors of large bandgap shows blue shift in photocurrent spectrum for the TE and TM mode with respect to that of small bandgap. It was shown that integrated photodetectors could demultiplex 1480 and 1550 nm wavelength. Photocurrent ratio was greatly enhanced by increasing the length of dummy waveguide between two photodetectors. For sufficiently long dummy waveguide, photocurrent ratio of 200 was seen at a wavelength of 1480 and 1550 nm. This area selective quantum well intermixing can be further applied to implementation of monolithic integration of optical devices on a chip.

5.REFERENCES

1. N. Uchida et al., " Low-cost high-performance hybrid WDM module integrated on a PLC platform for fiber-to-the-home", 22nd European Conference on Optical Communication, pp. 107-114, 1996
2. H. Nakajima, A. Leroy, and J. Charil, "Full-Duplex Performance Assessment of In-Line Transceivers Emitting at 1.3 μm and Receiving at 1.55 μm", IEEE Photon. Technol. Lett., Vol. 8, pp. 1561-1563, 1996
3. Yasuhiro Suzuki, Ryuzo Iga, Takeshi Yamada, Hideo Sugiura, and Mitsuru Naganuma, "Crosstalk Characteristics of a 1.3-μm/1.5-μm Wavelength Demultiplexing Photodetectors Using Laser-Assisted MOMBE Growth", Journal of Lightwave Technol., Vol. 17, pp. 483-489, 1999
4. D. Moss, F. Ye, D. Landheer, P. E. Jessop, J. G. Simmons, H. G. Champion, I. Templeton, and F. Chatenoud, "Ridge Waveguide Quantum-Well Wavelength Division Demultiplexing Detector with Four Channels", IEEE Photon. Technol. Lett., Vol. 4, pp.756-759, 1992
5. A. N. M. Masum Choudhury, P. Melman, A. Siletti, Emil. S. Koteles, B. Foley, and B. Elman, "Metal-Semiconductor-Metal Demultiplexing Waveguide Photodetectors in InGaAs/GaAs Quantum Well Structures by Selective Bandgap Tuning", IEEE Photon. Technol. Lett., Vol. 3, pp. 817-820, 1991
6. Sang Ki Si, Deok Ho Yeo, Kyung Hun Yoon and Sung June Kim, " Area Selectivity of InGaAs-InP Multiquantum Well Intermixing by Impurity-Free Vacancy Diffusion" IEEE J. Sel. Top. Quantum Electron. Vol. 4, pp. 619-623, 1998
7. Deok Ho Yeo, Kyung Hun Yoon and Sung June Kim, "Characteristics of intermixed InGaAs/IngAAsP Multi-Quantum Well structure", Jpn J. Appl. Phys. Vol. 39, pp. 1032-1034, 2000
8. Xiucheng Wu, Paul E. Jessop, Doug M. Bruce, Brad J. Robinson, and David A. Thompson, "Inline Quantum-Well Waveguide Photodetectors for the Measurement of Wavelength Shifts", J. Lightwave Technol., Vol. 15, pp. 2278-2283, 1997